Precise *in situ* tuning of the critical current of a superconducting nanowire using high bias voltage pulses

2011 Nanotechnology 22 395302

(http://iopscience.iop.org/0957-4484/22/39/395302)

Nanotechnology **22** (2011) 395302 (7pp) doi:10.1088/0957-4484/22/39/395302

Precise *in situ* tuning of the critical current of a superconducting nanowire using high bias voltage pulses

Thomas Aref and Alexey Bezryadin

University of Illinois at Urbana-Champaign, 1110 West Green Street Urbana, IL 61801, USA

E-mail: bezryadi@illinois.edu

Received 13 May 2011, in final form 4 August 2011
Published 5 September 2011
Online at stacks.iop.org/Nano/22/395302

Abstract

We present a method for *in situ* tuning of the critical current (or switching current) and critical temperature of a superconducting MoGe nanowire using high bias voltage pulses. Our main finding is that as the pulse voltage is increased, the nanowire demonstrates a reduction, a minimum and then an enhancement of the switching current and critical temperature. Using controlled pulsing, the switching current of a superconducting nanowire can be set exactly to a desired value. These results correlate with *in situ* transmission electron microscope imaging where an initially amorphous nanowire transforms into a single crystal nanowire by high bias voltage pulses. We compare our transport measurements to a thermally activated model of Little's phase slips in nanowires.

(Some figures in this article are in colour only in the electronic version)

Superconducting nanowires have unique superconducting properties due to their one-dimensional nature. They have been proposed as candidates for device applications such as various solid state qubit implementations [1–3] and as photon counters [4]. We describe a post-fabrication technique using high bias voltage pulses that allows precise *in situ* control over the critical current of a superconducting nanowire and explain a counterintuitive enhancement of the critical current observed with higher pulse voltages.

We have performed experiments applying controlled high bias pulses to superconducting MoGe nanowires *in situ*. We observed a decrease of switching current, I_{SW}, which is measured at a fixed temperature, typically 0.3 K. Analysis of the rate of Little's phase slips indicates that pulsing also causes a decrease in the critical temperature, T_C, of the wire. Initially, the wire maintains an overall behavior consistent with being a homogeneous nanowire with a reduced switching current and critical temperature but no significant change in the normal resistance. As larger and larger pulses are applied, the switching current reaches a minimum and then starts to increase, returning to values similar to or exceeding the starting switching current. Critical temperature also returns and normal resistance is observed to drop. Using scanning electron microscope (SEM) and transmission electron microscope (TEM) analysis, we find that this is a permanent morphological change of the nanowire and not weak link formation.

An interesting application of this effect is to control the switching current of a superconducting nanowire, opening the possibility of *in situ* engineered nanowires with precise switching currents (and to a lesser extent critical temperatures). We demonstrate that the switching current can be set to within approximately 10 nA of a desired value (see figure 1). The switching current cannot be more accurately defined as its natural stochastic behavior results in a distribution with a standard deviation of the order of 10 nA [5].

The nanowires were fabricated using the method of molecular templating [6]. Briefly, fluorinated single wall carbon nanotubes (SWNTs) were suspended across a trench in a Si substrate coated with SiO_2 and SiN films. $Mo_{76}Ge_{24}$ is deposited by DC sputtering forming a nanowire by using the nanotube as a nanoscaffold. Pattern definition by photolithography and the undercut of the trench allow only one conductance path, the nanowire, to be formed. The superconducting properties of the nanowires were measured in a He-4 (base temperature 1.5 K) or He-3 system (base temperature 0.3 K). The nanowires were measured in a standard current biased setup with a low noise voltage source

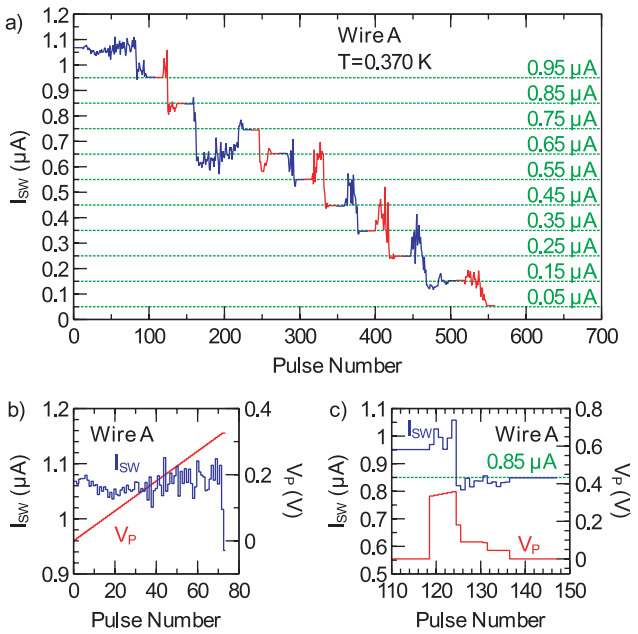

Figure 1. (a) I_{SW} can be set exactly using a combination of large and small pulses. The flat regions correspond to the set value of I_{SW} where no pulsing is applied. The noisy regions correspond to I_{SW} being set to the desired value as pulsing is applied. In this example, the starting I_{SW} was 1.07 μA and the chosen target values are shown by the green dotted lines. The pulse number represents the ordering of pulses in time and is not proportional to the pulse amplitude. Some pulses have zero amplitude, namely those corresponding to the plateaus of I_{SW}. (b) Close-up of the effect of pulsing on I_{SW} as V_P is increased from 0 to 0.326 V. As V_P grows, I_{SW} becomes increasingly stochastic until at large enough pulses we observe a strong downward trend. In this case, the drop in I_{SW} occurs at pulse number 73 for $V_P = 0.326$ V. (c) Setting of I_{SW} to 0.85 μA with accompanying voltage pulses. At first large pulses are applied to get I_{SW} near the desired value. Then smaller pulses are applied to bounce the I_{SW} to the exact value desired.

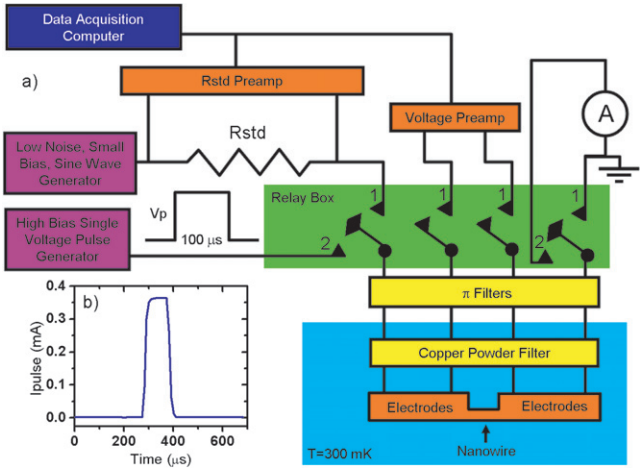

Figure 2. Experimental setup: (a) four relays (voltage controlled switches) are used to switch between measurement and pulsing mode. In measurement mode (all relays in position 1), we can measure either voltage versus current curves (amplitude of current ≈1–10 μA) or resistance versus temperature curves (amplitude of current ≈10–20 nA). A sine wave generator connected through $R_{std} = 0.1$–1 MΩ forms a current source connected to the left lead. A small voltage (≈1–10 mV) is measured on the two center leads. The right current lead is grounded. In pulsing mode (relays in position 2), a single high bias voltage pulse (≈0.1–1 V) is sent in on the left current lead, the two center leads are disconnected and the pulse can be detected on the right lead using an ammeter (≈0.1–1 mA). (b) Example measured current going through nanowire from a high bias voltage pulse measured with the ammeter. The pulse is 100 μs long and there are minor amounts of rounding of the pulse due to filtering in the cryostat.

feeding a large value standard resistor R_{std} serving as a current source and separate voltage probes.

The four-probe measurement is of the superconducting electrodes in series with the nanowire, not just the nanowire itself. The electrodes go superconducting at a temperature considerably higher than the nanowire does and they are also seamlessly connected to the nanowire so the contact resistance is zero. Thus the performed measurements give the resistance of the wire only. We name this type of arrangement of the current and voltage probes a quasi-four-probe measurement. In order to protect sensitive measurement equipment from high bias pulses (1 V or more) and to allow application of a voltage bias rather than a current bias pulse, a switching system was employed to switch between measurement mode and pulsing mode (see figure 2(a)). In order to study the effect of voltage pulsing, the wire was pulsed between sensitive measurements but not during the measurements.

Both manually operated switches and automated relays (voltage powered switches controlled by a computer) were used. No difference in behavior of the nanowires was observed between the two. The relays were low bias, latching relays powered by a Keithley electrometer controlled by the measurement computer through a general purpose interface bus. The latching design of the relays allows the power to the relays to be removed without affecting the switch position of the relays. To test the relays, repeated switches were made with no pulse application. No effect on any nanowire was observed from just switching back and forth without pulse application. Square pulses were applied using a data acquisition (DAQ) card. Pulse duration was kept at 100 μs and pulse voltage amplitude was varied. Pulses of this length transmit fairly well through the filtering system on the cryogenic measurement systems, maintaining their square shape with minimal rounding (see figure 2(b)). We have not systematically explored the effect of different length pulses (or different shaped pulses) but we do not expect significant dependence on these two factors for the following reasons. The response time of the nanowire should be of the order of picoseconds (the capacitance of the electrodes is of the order of a few fF [7] while the resistance is approximately 1 kΩ giving a RC time constant of approximately 1–10 ps) so the wire will have reached equilibrium current early in the pulse. The wire is expected to reach its maximum temperature (due to Joule heating) during the pulse and cool back to base temperature after the pulse within 10–100 ns [5] so it should be well thermally equilibrated early in the pulse as well. It should be noted that our relay switching speed (it takes approximately 1 s for the relay to switch between modes) is not fast enough to allow us to capture the cooldown back to base temperature after

the pulse and the wire is well thermalized before switching currents are measured after a pulse.

In measurement mode, a low bias sine wave signal current source is applied to the nanowire and the voltage is measured separately using the quasi-four-probe measurement described previously (see figure 2(a)). Typical voltage versus current (*VI*) curves and the effects of pulsing on them are shown in figure 3. I_{SW} initially decreases with minimal change in R_N and I_R and the *VI* curves maintain single hysteretic loops characteristic of homogeneous wires. The hysteresis in the *VI* curve disappears as the switching current goes to a minimum (see figure 3(d)). A flat, superconducting region indicates that a non-zero critical current always remains. Higher pulsing results in a return of the hysteretic *VI* curve with now increasing I_{SW} and decreasing R_N as the pulse voltage is increased. When I_{SW} returns, we generally observe phase slip centers in the *VI* curves (see figure 3(e)) indicating less homogeneous nanowires. As pulse voltage is further increased, these phase slip centers gradually disappear. The wire can return to a I_{SW} approaching the starting I_{SW} (see figure 3(b)) or even exceeding it (see figure 3(f)). From these types of *VI* curves, we can extract the switching current, I_{SW}, using threshold detection and the normal resistance, R_N, using linear fitting and plot the data versus pulse number or pulse voltage, V_P, across the nanowire. The effect as V_P is increased from 0 to 0.326 V in 5 mV steps is shown in figure 1(b). For the lowest voltage pulses, we primarily observe scatter from the natural stochasticity of the switching current [5]. In order to minimize this natural stochasticity, we averaged over 100 switching current measurements between pulses. As V_P is increased, we observe an increasing stochasticity of I_{SW} which quickly becomes greater than the natural stochasticity of the switching current. As the pulse voltage increases further, we see the irreversible drop of the switching current observed in the *VI* curves. It should be noted that I_{SW} was always measured sufficiently long after the voltage pulse was finished that the wire had time to completely equilibrate to the bath temperature. Thus the observed changes in I_{SW} are due to the voltage pulse permanently altering the wire and not the heating effects of the high bias pulse. We can use this combined downward trend and increased stochasticity to precisely set I_{SW} to a desired value. As shown in figure 1(a), I_{SW} is set to 10 values chosen uniformly from 0.95 to 0.05 μA. An example of a pulse sequence used to do this is shown in figure 1(c). Large pulses are used to approach the desired value and then smaller pulses (with their enhanced stochasticity) are used to 'bounce' the switching current to within $\approx$10 nA of the desired value. For each of the 10 chosen target values, the switching current was set to the desired value.

The decrease and return of I_{SW} seen in the *VI* curves can be plotted versus V_P in a similar fashion. It should be noted that as the switching current goes through its minimum it is poorly detected by this threshold detection scheme. The drop, saturation and return of I_{SW} can be seen in figure 4. The initial drop of I_{SW} does not have a corresponding change in R_N. When I_{SW} reaches a minimum and begins to return, R_N begins to drop. This behavior was consistent for all nanowires measured and was reproduced on many nanowires (of which figure 4 contains four examples).

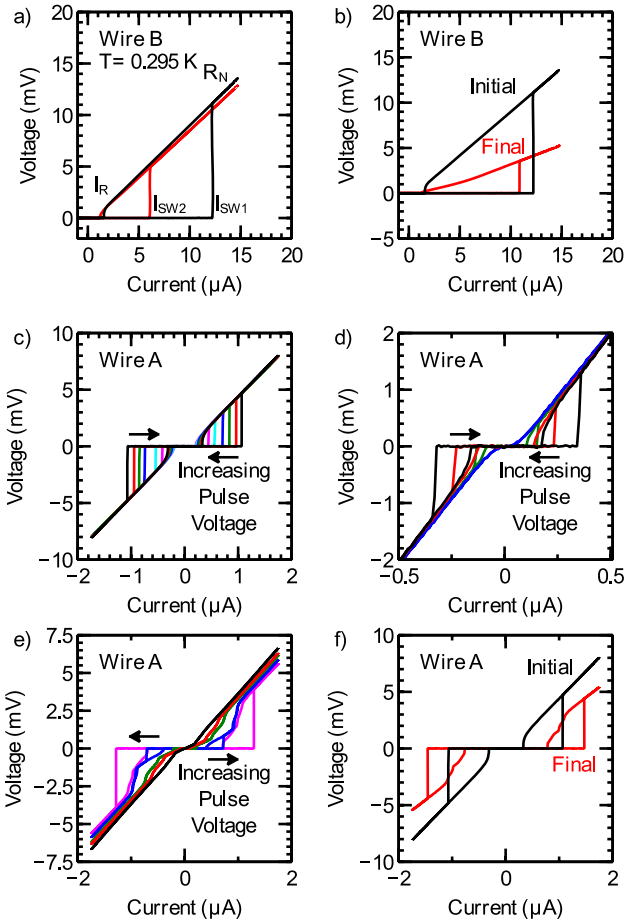

Figure 3. Voltage versus current (*VI*) curves demonstrating the effect of high bias pulses. (a) Initial application of high bias pulses decreases the switching current from I_{SW1} to I_{SW2} while minimally changing R_N and I_R. (b) Further pulsing results in the return of I_{SW} and a drop in R_N. 'Initial' is the same curve as the one shown in black in graph (a). 'Final' is the last *VI* curve before the sample broke. (c) A different nanowire with a smaller initial I_{SW}. This graph shows many *VI* curves to indicate the gradual decrease of I_{SW} as increasing pulses are applied. (d) Application of higher pulses results in a loss of hysteresis of the *VI* curve. However, the *VI* curve retains a flat, superconducting region with apparently non-zero critical current. (e) Still higher pulses results in the return of I_{SW} with a drop in R_N and evidence of phase slip centers. (f) Still higher pulsing produces an almost uniform *VI* curve with I_{SW} exceeding the original switching current and a further drop in R_N. 'Initial' is the same curve as the one shown in black in (c). 'Final' is the last *VI* curve before the sample broke.

The resistance versus temperature curves taken after a series of pulsing (see figures 5(a) and (b)) show behavior consistent with the observed I_{SW} and R_N behavior (for the *RT* curve, the low bias current signal was reduced from $\approx$1–10 μA to 10–20 nA to measure the *RT* curve in the linear regime). The *RT* curves generally demonstrate one transition indicative of a homogeneous wire with fitting parameters similar to unpulsed nanowires. The critical temperature, T_C, of the nanowire decreases as pulse voltage increases saturating at a minimum. T_C is defined as a fitting parameter in the best Little fit (discussed in detail below). Further increase of pulse voltage results in the increase of T_C and the drop in R_N (see figures 5(c) and (d)).

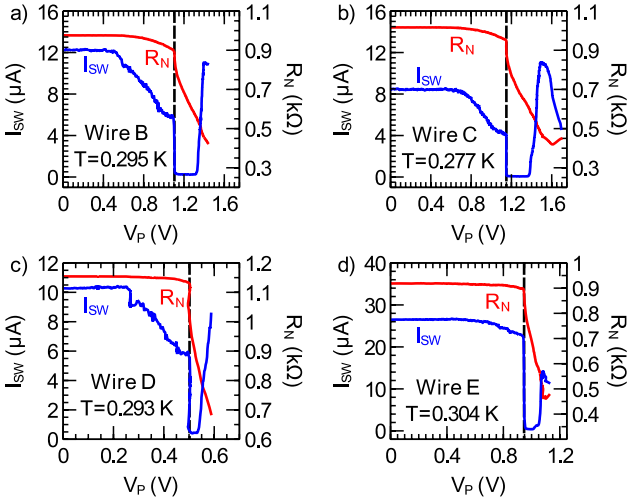

Figure 4. Switching current, I_{SW}, and normal resistance, R_N, versus the maximum pulse voltage, V_P, applied to the wire. The blue line is I_{SW} which decreases and then increases with increasing pulse amplitude. The red line is R_N, which stays constant and then decreases. This is a counterintuitive result that was consistent on all nanowires measured and has been reproduced on several nanowires of which (a), (b), (c) and (d) are four examples. The dashed line indicates where both R_N and I_{SW} begin to rapidly decrease. Applying pulses smaller than the maximum previous applied pulse does not lead to a significant change in I_{SW}. (a) A nanowire with starting $I_{SW} = 12.2\ \mu$A. The dashed line is at 1.105 V. I_{SW} returns to 11.0 μA before the wire abruptly breaks. (b) A wire with similar fabrication parameters to the one shown in (a) (the axes are the same for graphs (a) and (b)). The starting $I_{SW} = 8.5\ \mu$A. The dashed line is at 1.150 V. I_{SW} returns to a maximum of 10.9 μA (which is greater than the starting I_{SW}) before decreasing again until the wire breaks. (c) A third example nanowire with starting $I_{SW} = 10.3\ \mu$A and ending $I_{SW} = 8.5\ \mu$A. The dashed line is at 0.502 V. Images of this wire before and after pulsing are shown in figure 6. (d) A nanowire fabricated on a multi-walled carbon nanotube instead of a fluorinated SWNT with starting $I_{SW} = 26.5\ \mu$A and ending $I_{SW} = 11.4\ \mu$A. The dotted line is at 0.947 V.

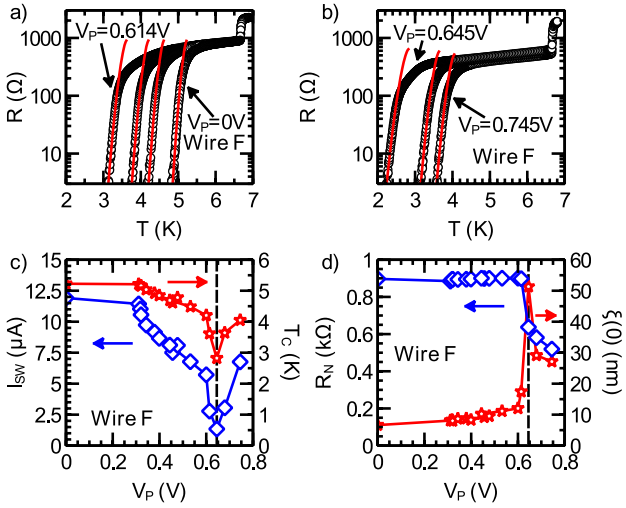

Figure 5. Resistance versus temperature curves and fits. (a) Four RT curves taken as pulsing generally drives I_{SW} down. From right to left, the corresponding pulse voltages are 0, 0.456, 0.600 and 0.614 V. The red curves are best fits to a thermally activated phase slip model. (b) Three RT curves taken when I_{SW} returns for the same wire as shown in (a). From left to right the pulse voltages are 0.645, 0.679 and 0.745 V. (c) I_{SW} and T_C versus V_P for the wire whose RT curves are shown in (a) and (b). The diamonds correspond to I_{SW} and the stars correspond to T_C. The dotted line is at 0.645 V where the turnaround from decreasing to increasing behavior occurs. (d) R_N and $\xi(0)$ versus V_P. The diamonds correspond to R_N and the stars correspond to $\xi(0)$. Initially R_N is flat while $\xi(0)$ shows a growing trend. After V_P reaches 0.645 V, R_N begins to drop and $\xi(0)$ shows a maximum and saturates to a value higher than the starting value.

SEM imaging (figures 6(a) and (b)) before and after pulsing show virtually no change in the nanowire, ruling out the formation of obvious weak links. To more thoroughly study the effect of pulses on the nanowires, we turn to *in situ* TEM experiments. TEM experiments require different samples from those described previously. Most importantly, the nanowire must be across an open slit for TEM observation. We deposit multi-walled carbon nanotubes (MWNTs) across TEM compatible slits to generate these samples [8]. MWNTs were used for the TEM samples (instead of the SWNTs used for non-TEM compatible samples described above) because MWNTs are more robust and rigid and can thus more easily be deposited on the TEM compatible slits (the SWNTs tend to sag into the TEM slits and not produce suitable nanowires). The MWNT scaffold makes for a less ideal wire than a SWNT since the diameter of the MWNT (approximately 20 nm) is comparable to the thickness of the metal film deposited to form the nanowire while the diameter of the SWNT is much smaller (approximately 2 nm). The MWNTs may also contribute some shunt conductance so SWNTs were preferred when feasible. The SWNTs are fluorinated to make them fully insulating so they do not contribute a shunt conductance to the resistance measurement (i.e. the measurement is completely dominated by the superconducting wire). The change in scaffold does not affect the pulsing behavior (see figure 4(d)).

The TEM compatible slits are formed using a KOH etch to fabricate a V-shaped cut in a silicon chip coated on both sides with 100 nm of silicon nitride. The V-shaped cut almost pierces the chip except for approximately 5 μm of remaining silicon. This silicon is cracked by sonicating in deionized water for less than a second. A 30–60 s KOH etch removes the cracked silicon leaving an approximately 100 nm wide silicon nitride membrane. This membrane is removed by reactive ion etching (RIE) from the etch pit side. The membrane is supported during the RIE step by a piece of polydimethylsiloxane (PDMS). In the method previously described [8] we removed the silicon nitride entirely and oxidized the silicon to form an insulating layer. By etching the silicon nitride from the etch pit side, we are able to use the silicon nitride as the insulating layer, thus skipping the oxidizing step. With these samples, we were able to perform *in situ* TEM experiments to directly determine the effects of high bias voltage pulses on metal coated nanotubes. The *in situ* TEM experiments must be done at room temperature while superconducting measurements must be done at cryogenic temperatures. We do not expect this change in base temperature to produce a significant difference as both experiments are performed under vacuum and the nanowire itself is expected to reach a high temperature (≈2000 K) under a high bias voltage (≈0.5 V).

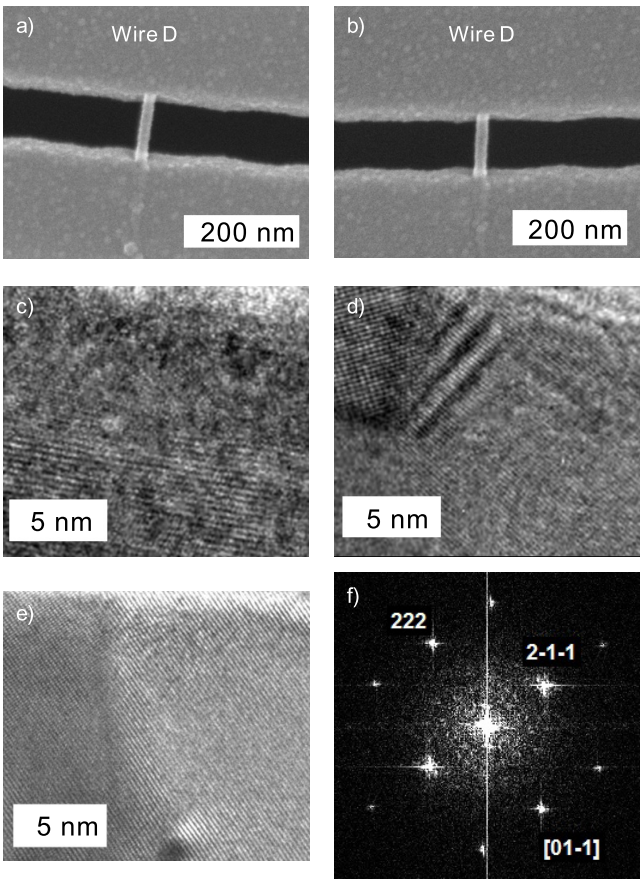

Figure 6. SEM and TEM analysis: (a) SEM image of a nanowire before pulsing at cryogenic temperatures and (b) the same nanowire as (a) after pulsing at cryogenic temperatures with a maximum pulse voltage applied of 588 mV. The switching current of the wire was reduced from 10.3 μA down to a minimum and then back to 8.5 μA as shown in figure 4(c). Note no obvious weak links are visible. (c) *In situ* TEM imaging of a nanowire (at room temperature) exposed to pulsing. Before pulsing, the nanowire is amorphous (the crystalline structure visible is the underlying MWNT). (d) After pulsing to 2.935 V, the wire becomes polycrystalline. (e) After pulsing to 3.735 V, the nanowire becomes a single crystal. (f) Electron diffraction pattern of the crystal shown in (e) used to determine crystal orientations.

From the *in situ* TEM experiments we see that initially the wire develops a polycrystalline section which expands as increasing pulses are applied. The crystals do not necessarily remain static for the duration of the experiment but rather are dynamic entities that develop and change. The polycrystalline nature of the wire gradually becomes dominated by fewer and fewer crystal domains and becomes an almost perfect single crystal nanowire. It should be noted that although inhomogeneities such as grain boundaries appear in the wire, the overall diameter of the wire does not appear to be significantly altered. The crystallization of MoGe from a high voltage pulse is not surprising in light of similar crystallization obtained by exposure of MoGe nanowires to electron beam radiation [9]. To avoid electron beam induced crystallization in our TEM images, dosage from the electron beam was minimized for all TEM images. As further evidence that the high bias pulses and not the electron beam of the TEM were responsible for the crystallization observed, the same crystallization was seen in nanowires constantly imaged during the pulse process as was seen in wires that were not imaged until the pulse process was complete. In the first TEM image, the multi-walled nanotube (with wall spacing 3.3 Å) covered with amorphous $Mo_{76}Ge_{24}$ is visible (see figure 6(c)). The measured line spacing in the image is 3.2 ± 0.1 Å which corresponds to the underlying nanotube. After some pulsing, a polycrystalline structure is visible with the predominant line spacing being 2.2 ± 0.1 Å. Only in the upper left hand corner is the line spacing different 2.5 ± 0.1 Å (see figure 6(d)). In the final TEM picture the single crystal line spacing is 2.2 ± 0.1 Å (see figure 6(e)). Note that TEM imaging conclusively shows that weak links are not formed. The observed crystallization in the TEM agrees with the scanning electron microscope (SEM) imaging showing that pulsing makes the wire edges slightly less rough (figure 6(b)).

SEM and TEM imaging do not show any formation of weak links due to pulsing. Thus the reduction of the critical current cannot be explained by weak links and we need to find an alternative explanation. Note also that weak links would only account for the reduction of switching current and not explain the observed return of the switching current with increased pulse voltage. The dynamic, increased stochasticity of the critical current and the decrease and return of the critical current correlates well with the observed TEM behavior. Most forms of crystalline MoGe have lower T_Cs than amorphous MoGe [10] so it is not surprising that the crystallization of MoGe would reduce the wire's critical temperature. It can be expected that any crystallization or segregation of the MoGe alloy from the large current pulse would produce a reduction of T_C. TEM imaging shows that a polycrystalline morphology appears with voltage pulsing. Following the work of Rogachev *et al* [11], we can expect these polycrystalline wires to maintain homogeneous wire behavior and can fit them using standard nanowire theory. Also in agreement with these previous results, we see phase slip centers develop in the *VI* curve (see figure 3(e)) at temperatures near T_C (as we are changing T_C while keeping T fixed, these are most evident when T_C is small).

Electromigration is a well studied effect for modifying and fabricating nanostructures [12–14]. The observed crystallization of the MoGe is most likely caused by a combination of electromigration and Joule heating induced thermal effects. It appears that thermal effects are dominant since we observe the appearance of crystals at the center hottest spot of the wire and also do not observe the weak link formation associated with electromigration. As a rough approximation of the temperature of the nanowire, we can write the applied voltage as a function of temperature (assuming a constant resistivity): $V^2/4 = L(T^2 - T_0^2)$ where V is the voltage of the pulse, $L = 2.4 \times 10^{-8}$ W Ω K^{-2} is the Lorenz number, T is the temperature of the wire center and T_0 is the temperature of the electrodes [15]. Typical values ($V = 0.5$ V) gives us an estimated temperature of $T = 1725$ K close to the crystallizing temperature of MoGe. This high temperature further indicates that the difference between cryogenic temperatures $T_0 = 0$ and room temperature

TEM measurements $T_0 = 300$ K can safely be neglected. It should be noted that this rough approximation indicates that the natural choice of coordinates for figure 4 is pulse voltage (and not pulse current or power). The modification of critical temperature as a result of an applied voltage pulse is not surprising when one considers that the entire material properties of the nanowire may be changed. The particular crystal form of MoGe closest to our starting concentration of $Mo_{76}Ge_{24}$ is Mo_3Ge, which is actually an A15 compound; these are known to have high T_Cs. Studies on Mo_3Ge reveal that its T_C is highly dependent on the formation conditions (i.e. it can have a very low T_C) but under the correct formation conditions, the T_C can exceed 5.7 K (comparable to the critical temperature of the starting amorphous MoGe) [10].

By comparing x-ray diffraction data for Mo_3Ge [16] to our TEM images and electron beam diffraction data (figures 6(d)–(f)), we can confirm that Mo_3Ge is being formed by the pulses. In agreement with the x-ray diffraction data, our most commonly observed orientations are 210 (2.1993 Å from x-ray diffraction) and 211 (2.0031 Å from x-ray diffraction). Our measurement of 2.2 Å by electron microscopy is not accurate enough to tell the difference between these two orientations. From further analysis of the TEM images, we retrieve that the spacing of the crystal in the 222 direction is 1.5 Å (compared to 1.4215 Å from x-ray diffraction). For the 211 direction, we measure 2.1 Å (compared to 2.0031 Å from x-ray diffraction). On the upper left hand corner of the polycrystal, we observe a spacing of 2.5 Å (compared to 2.4557 Å from x-ray diffraction) for the 200 and 3.3 Å for the 110 direction (compared to 3.4724 Å from x-ray diffraction). Both these orientations are significantly less common than the others which dominate the images. In all cases, there is significant correlation between our values and the x-ray diffraction data, conclusively indicating that the crystal we are generating is indeed Mo_3Ge [16].

To compare to previous experiments on nanowires we use a phenomenological Little thermally activated phase slip (TAPS) model [17]: $R(T) = R_N \exp(-\Delta F(T)/k_B T)$ where R_N is the normal resistance of the nanowire, $\Delta F(T)$ is the free energy barrier for phase slips, k_B is the Boltzmann constant and T is temperature [17–20]. The temperature dependence of the free energy barrier is accurately given at all temperatures by the Bardeen formula [21]: $\Delta F(T) = \Delta F(0)(1-(T/T_C)^2)^{3/2}$ where we can express $\Delta F(0)$ using experimentally accessible parameters [22] as $\Delta F(0) = 0.83(R_Q/R_N)(L/\xi(0))k_B T_C$. R_Q is the resistance quantum, R_N is the normal resistance of the nanowire (which we define as the resistance immediately after the film goes superconducting), L is the length of the nanowire (which can be determined from SEM imaging), T_C is the critical temperature and $\xi(0)$ is the coherence length. This model is used to produce the fits shown in figure 5 where the fitting parameters are critical temperature, T_C, and coherence length, $\xi(0)$. The critical current, I_C is related to the free energy barrier, ΔF by $\Delta F = \sqrt{6}(\hbar/2e)I_C$ [22]. This indicates that a reduction in T_C would produce a reduction in I_{SW}.

As shown in figure 5(c), the decrease and return of I_{SW} corresponds to a drop and return of T_C as expected. In figure 5(d), we see that R_N is stable and coherence length is gradually increasing as would be expected from the corresponding decrease in T_C [19]. When I_{SW} saturates at a minimum and begins to increase, R_N starts to decrease. Likewise, the coherence length returns from a maximal value (the maximum being due to a highly reduced T_C) and approaches a value higher than its initial value. This is reasonable since as the wire becomes well-ordered crystalline Mo_3Ge, we anticipate an enhanced coherence length due to the longer mean free path of the crystal compared to amorphous MoGe. From a simple Drude model of resistivity, a longer mean free path also implies a decreased normal resistance, in agreement with the observed drop in resistance.

While the experimental results here are specific to MoGe, this method should be applicable to other superconducting metals. Nb has shown similar behavior to MoGe on exposure to electron beams [9] so it would not be surprising if it showed similar crystallization under high bias pulsing. It should be noted that the transport behavior seen might be significantly different. Crystallized Nb would not necessarily have a high T_C, and thus the return of superconductivity seen for MoGe would not be observed. As another example, Al is atomically much lighter than MoGe so it might well be dominated by electromigration (though Al also has a rather low melting point so this is not certain). The return of superconductivity with the highest pulse voltages is related to the chemical composition of the starting material. The correct starting mixture of amorphous materials might allow crystalline nanowires with high T_C to be formed. Example materials to aim for would be Nb_3Ge (another A15 compound with $T_C = 23$ K) [23] or MgB_2 (conventional superconductor with highest $T_C = 39$ K) [24].

In conclusion, we demonstrate that controlled high bias pulsing can be used to precisely set the switching current of the nanowire and that the counterintuitive decrease and increase of the switching current with increasing pulse voltage is well explained by crystallization induced by Joule heating.

Acknowledgments

We thank Jian-Guo Wen for help with the TEM analysis. This material is based upon work supported by NSF-DMR 10-05645 and by the US Department of Energy under grants DE-FG02-07ER46453 and DE-FG02-07ER46471 through the Frederick Seitz Materials Research Laboratory at the University of Illinois at Urbana-Champaign.

References

[1] Mooij J E and Harmans C J P M 2005 *New J. Phys.* **7** 219
[2] Mooij J E and Nazaron Y V 2006 *Nature Phys.* **2** 169
[3] Ku J, Manachurian V and Bezryadin A 2010 *Phys. Rev.* B **82** 134518
[4] Kerman A J, Dauler E A, Keicher W E, Yang J K W, Berggren K K, Gol'tsman G and Voronov B 2006 *Appl. Phys. Lett.* **88** 111116
[5] Sahu M, Bae M, Rogachev A, Pekker D, Wei T, Shah N, Goldbart P and Bezryadin A 2009 *Nature Phys.* **5** 503
[6] Bezryadin A, Lau C N and Tinkham M 2000 *Nature* **404** 971
[7] Bollinger A T, Rogachev A and Bezryadin A 2006 *Europhys. Lett.* **76** 505

[8] Aref T, Brenner M and Bezryadin A 2009 *Nanotechnology* **20** 045303
[9] Remeika M and Bezryadin A 2005 *Nanotechnology* **16** 1172
[10] Ghosh A K and Douglass D H 1977 *J. Low Temp. Phys.* **27** 487
[11] Rogachev A and Bezryadin A 2003 *Appl. Phys. Lett.* **83** 512
[12] Park H, Lim A, Alivisatos A, Park J and McEuen P 1999 *Appl. Phys. Lett.* **75** 301
[13] Strachan D R, Johnston D E, Guiton B S, Datta S S, Davies P K, Bonnell D A and Johnson A T C 2008 *Phys. Rev. Lett.* **100** 056805
[14] Heersche H B, Lientschnig G, O'Neill K, van der Zant H and Zandbergen H 2007 *Appl. Phys. Lett.* **91** 072107
[15] Holm R 1967 *Electrical Contacts* (Berlin: Springer)
[16] Searcy A W, Peavler R J and Yearian H J 1952 *J. Am. Chem. Soc.* **74** 566
[17] Bezryadin A 2008 *J. Phys.: Condens. Matter* **20** 043202
[18] Chu S L, Bollinger A T and Bezryadin A 2004 *Phys. Rev.* B **70** 214506
[19] Tinkham M 1996 *Introduction to Superconductivity* (New York: Dover)
[20] Langer J S and Ambegaokar V 1967 *Phys. Rev.* **164** 498
[21] Bardeen J 1962 *Rev. Mod. Phys.* **34** 667
[22] Tinkham M and Lau C N 2002 *Appl. Phys. Lett.* **80** 2946
[23] Gavaler J R, Janocko M A and Jones C K 1974 *J. Appl. Phys.* **45** 3009
[24] Nagamatsu J, Nakagawa N, Muranaka T, Zenitani Y and Akimitsu J 2001 *Nature* **410** 63